Visual Observation and Modeling of the Foaming of Thermoplastics by Supercritical Carbon Dioxide.

Yoshinobu Ozaki[1], Katsuto Otake[*2], Satoshi Yoda[2], Yoshihiro Takebayashi[2], Tsutomu Sugeta[2], Noriaki Nakazawa[2], Hideki Sakai[1], Masahiko Abe[1]
1: Faculty of Science and Technology, Tokyo University of Science, Yamazaki 2641, Noda, Chiba 278-8510, Japan
2: National Institute of Advanced Industrial Science and Technology, Institute for Green Technology, Higashi 1-1-1, Tsukuba Central 5, Tsukuba, Ibaraki 305-8565, Japan
e-mail: katsuto-otake@aist.go.jpp, Phone/Fax: +81-298-61-4567

ABSTRACT: For the *in situ* observation of the foaming of thermoplastics by depressurization of supercritical carbon dioxide, high-pressure thin layer view cell was constructed. With using poly(propylene) sheets as samples, initial stage of the rate of cell diameter growth and cell number increase were measured with changing temperature, pressure, and pressure release rate. The initial cell nuclei were formed within the initial several seconds, and the number of the cell does not change in the successive cell diameter growth process. The cell diameter increasing rate was most rapid in the initial cell nuclei formation period, and slowed down in the cell growth period. These physical phenomena were attempted to explain through the nucleation theory.

I. INTRODUCTION

Microcellular plastics are polymeric foamed materials characterized by cell sizes in the range of 0.1 to 10 micrometers, number of the cells in the range of 10^9 to 10^{15} cells per cubic centimeter, and void ratio in the range of 5 to 98 % [1,2] In the early 1980's, Suh *et al.* reported a new processing method forms this microcellular plastics [3]. The process consists of two steps, formation of gas (blowing reagent) supersaturated mixture of polymers followed by the induction of thermodynamically unstable state which causes nucleation and growth of bubbles in the mixture.

In many cases, microcellular plastics have better thermal and electrical properties compared with the neat polymers and plastic forms made by conventional methods [1, 2], and in some cases, they also have better mechanical properties [4, 5]. Moreover, the new process has an environmental advantage over the conventional foaming processes, because natural working fluid such as carbon dioxide (CO_2) and nitrogen are used as the blowing gases instead of hydrocarbons, chlorofluorocarbons, hydrochlorofluorocarbons, and toxic organic solvent [6, 7]. Therefore, the process is a highly expectative for the reduction of amount of polymeric materials used in a given part without sacrificing any physical properties, and giving any other environmental impact.

From the first report of Suh *et al.*, many efforts have been made for the full understanding of the controlling factors of the foaming process as well as the structure of foamed materials [8-19]. However, it seems that the precise control of the final products is not achieved yet because of the complex conjunction of many factors such as solubility of gases, viscosity of the mixtures, and the rate of depressurization, which strongly conjugated each other. Even for the very first stage of the bubble nucleation, instead of the homogeneous and heterogeneous nucleation process, the possibility of the occurrence of spinodal decomposition was recently pointed out [20, 21], which seems to be experimentally supported by Oshima *et al*. [22]

In this study, *in situ* observation of initial bubble nuclei formation and successive bubble growth were measured during the initial several tens of seconds.

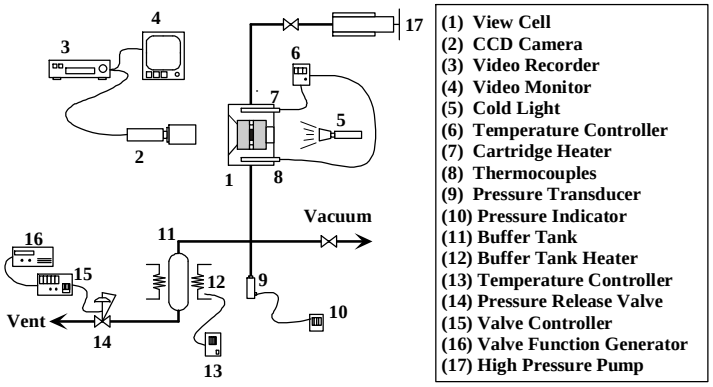

Figure 1. Schematic figure of experimental apparatus.

II. EXPERIMENTAL

(1)MATERIAL:

Poly(propylene) (PP) (Chisso Petrochemical Co., foam grade FH3400) was used as a polymer sample for this study.

(2) APPARATUS: Figure 1 shows the schematic diagram of experimental apparatus. Pressure of the system is controlled by a back pressure regulator (JASCO, 880-81) equipped with an external function generator (Hokuto Denko, HB-104) that enables the variation of pressure with time. A buffer tank (25cm^3 in volume) is for the system to stabilize the pressure. Temperature of the view cell is maintained by four cartridge heaters and a controller (Shimaden, DSM-T.C.U.). Accuracy of the temperature and pressure are well within 0.1K and 0.1MPa, respectively. The temperature of the buffer tank is maintained at 120^{o}C. The behavior of bubbles in the molten polymer during the depressurization operation are recorded with a digital video device (SONY DVCAM DSR-30) with a CCD camera (Sony, XC-79). The motion pictures are analyzed with NIH-image by downloading to a computer via an image capture board (CANOPUS DVRaptor 2000). The durable pressure and temperature of this apparatus are 30MPa and 170^{o}C, respectively.

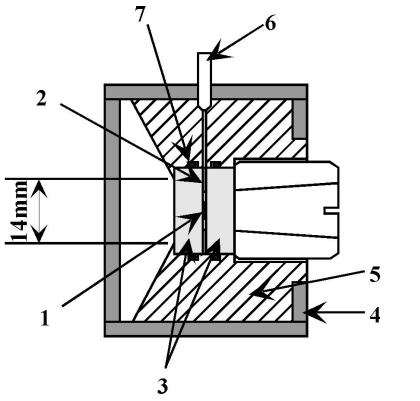

Figure 2. Schematic figure of the thin layer view cell.

Figure 2 shows the schematic figure of the view cell (Tama Seiki, H-06). The thin layer view cell had two sapphire windows separated by a C-shape stainless steel spacer of 0.5mm in thickness. The effective diameter of the glass was 14mm.

(3) Procedure: The PP disk of 0.5mm in thickness and 10 mm in diameter was fixed between the two sapphire plate. After several hours of the evacuation, temperature and pressure were razed to the experimental condition, and the samples were saturated with the CO_2 for 17 hours. Pressure was then released at constant rate (0.32MPa/s, 0.16MPa/s, 0.08MPa/s and 0.016MPa/s) to the atmospheric pressure. Therefore, the experiments were conducted by the constant-temperature variable-pressure method, and the experimental results would be analogous to the volume expansion of infinite rod.

III. Results and discussion

At first, foaming condition was determined. **Figure 3** shows the results of foaming condition determination [23]. From the figure, experimental condition was determined as saturation temperature= 160 and 180^{o}C, saturation pressure =15, 20 and 15 MPa, and

depressurization speed = 0.16-0.64 MPa/s.

Figure 4 shows typical images obtained in this study (Saturation temperature and pressure were 433.15K and 25MPa, pressure release rate was 0.64 MPa/s). Just after the pressure release, bubble (black dots in the figure) nuclei were formed, and grew with time. From these images, rate of bubble nuclei formation and rate of bubble growth with time was evaluated.

Figure 5 shows effects of pressure release rate on the bubble nuclei formation (a) and bubble growth (b) with time. In the figre, the slope of the bubble radius increase represents bubble growth rate. The timing of the bubble nuclei formation depended on pressure release rate, and slower the release rate, later the nuclei formation. The number of bubbles increased with time, and became constant. The radius of bubbles increased with time, and the growth of the bubble was clearly separated in two stages. At the initial stage, the growth rate of the bubble was almost independent of the pressure release rate. On the other hand, in the later stage, the growth rate became faster with decreasing the release rate. At the

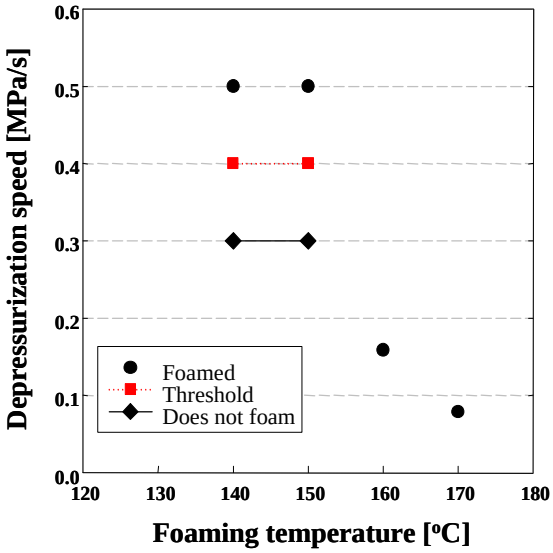

Figure 3. Relationship between foaming temperature and depressurization speed (Saturation pressure and Time: 10MPa, 15hrs)

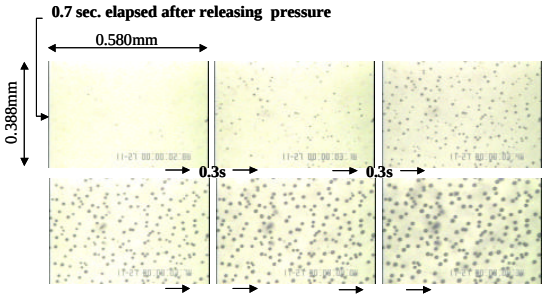

Figure 4. Continuous images during the foaming process. (Saturation temperature and Pressure : 433.15K, 25MPa ;Pressure release rate : 0.64 MPa/s)

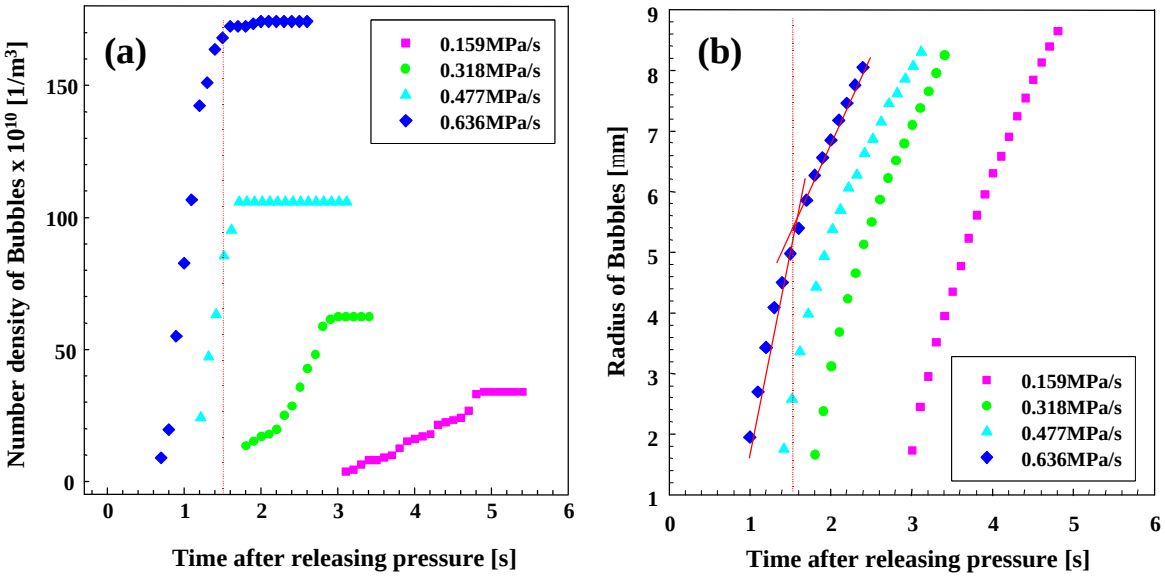

Figure 5. Effects of pressure release rate on the number of bubbles and radius of bubble. (433.15K, 25MPa)

same time, as shown in the figure by a dotted lines, the point of time when the growth rate changes agreed with that the formation of nuclei stopped. Cleary the bubble growth mechanism changes at the point of time.

Figure 6 shows rate of nucleation that obtained from the numerical derivative of the increase of the number density of bubbles. As could be seen in the figure, the nucleation rate has a maximum.

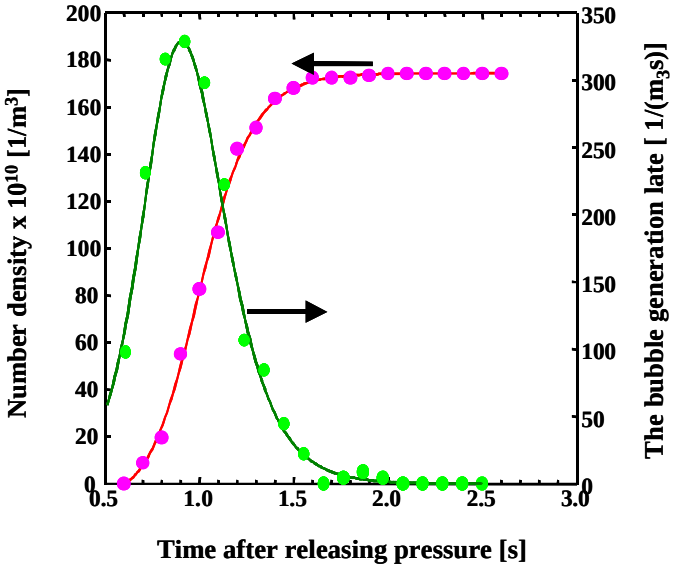

Figure 6. Rate of nucleation. (Saturation temperature and pressure were 433.15K and 25MPa, pressure release rate was 0.636MPa/s)

A typical foaming process involves several steps as saturation, nucleation, growth of the nucleated bubbles, and quenching of the foamed polymer. Among these steps, bubble nucleation is the most important that determines the structure of foams. In many cases, as the direct observation of initial nuclei formation is difficult, the formation of initial nuclei of the bubbles were treated as the nucleation from the homogeneous mixture by supersaturation. For the case of classical nucleation theory, the rate of nucleation could be expressed as follows:

$$J \propto \exp\left(-\frac{16ps^3}{3R^3T^3(\Delta S)^2}\right) \tag{1}$$

where J the nucleation rate, R the gas constant, T the temperature, s the surface tension, and ΔS the degree of supersaturation. For the consideration of the initial nucleation process, following facts were assuming ed: (1) experimental observation were performed at the center of polymer disk sample, (2) the sample could be approximated by an infinite rod, (3) the pressure inside and outside the sample is identical, (4) concentration of the gas depends on the pressure, and (4) diffusion of gas occurs only from the outer side interface of the sample.

In equation (1), the surface tension of PP/CO_2 is independent of pressure at constant temperature [24]. Assuming that the diffusion coefficient of CO_2 in PP is also independent of pressure at constant temperature [25], the concentration in the sample could be calculated by the following diffusion equation:

$$c(r,t) = k\left(t - \frac{a^2 - r^2}{4D}\right) + \frac{2k}{aD}\sum_{n=1}^{\infty}\exp\left(-Da_n^2 t\right)\frac{J_0(ra_n)}{a_n^3 J_1(aa_n)} \tag{2}$$

where $C(r,t)$ the concentration of CO_2 at radial position r and t seconds after the depressurization, k the rate of depressurization given by $P = P_0 - kt$, a the radius of the sample, D the diffusion coefficient of CO_2 in PP, and J the Bessel functions. **Figure 7** shows the concentration of CO_2 at the center of the sample. From the figure, it is clear that concentration change due to the diffusion of CO_2 from the sample could be neglected. Because the solubility of CO_2 depends on the pressure, degree of supersaturation ΔS increases with time as the pressure outside the sample decreases with time. **Figure 8** shows

the rate of nucleation calculated following the classical nucleation theory. From figures 6 and 8, it is clear that the rate of nucleation completely different from each other. This facts clearly shows that the initial nucleation that controls the foam structure does not follow the classical nucleation theory. As recent several reports suggested, the might be follow the spinodal decomposition. The nucleation rate shown in figure 6 seems to be follows the theory of spinodal decomposition.

IV. CONCLUSION

In this study, fundamental aspects of the microcellular forming process were examined with the high-pressure thin layer view cell for the *in situ* measurement. It was revealed that the initial bubble growth could be separated distinct two stages. Experimental results of the rate of the initial bubble nuclei formation were compared with the theoretical classical nucleation theory. It became clear that the mechanism of initial nucleation of bubbles is not follows the classical theory. As recent several reports suggested, it might be follows the spinodal composition of mixture of PP and CO_2.

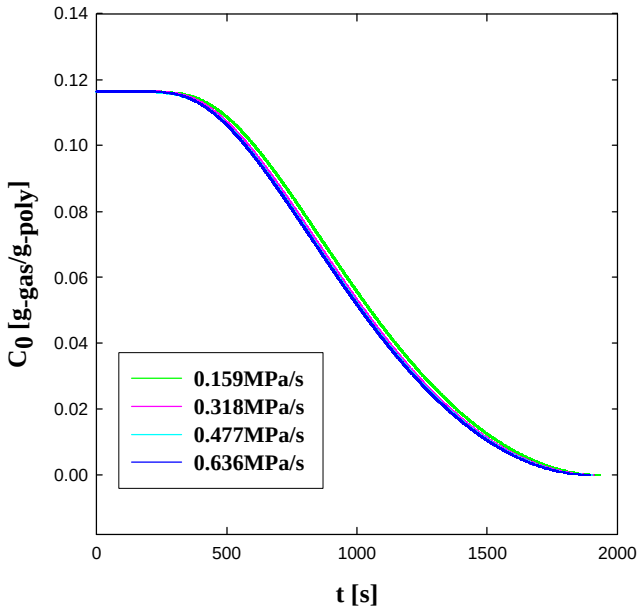

Figure 7. Concentration of CO2 at the center of the PP disk. (D=3.43x10^{-9} [m/s^2])

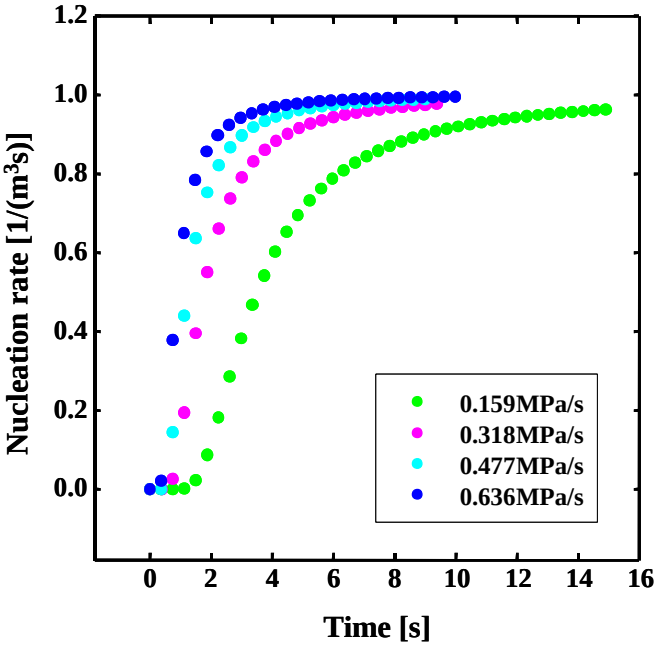

Figure 8. Nucleation rate theoretically calculated from equation (1).

ACKNOWLEDGEMENT

We thank Mr. Hideo Ohyabu for his help for revealing the optimum condition for foaming. We also thank Dr. Yoshiyuki Sato of Hirosima University for his permission to use the diffusion coefficient and solubility data. We thak Dr. Katsumi Tanaka of AIST for his help in calculation.

REFERENCES

[1] Baldwin, D. F.; Tate, D. E.; Park, C. B.; Cha, S. W.; Suh, N. P. Microcellular Plastics Processing Technology (1). *Seikei-Kakou* Vol.6, **1994**, pp. 188-194.

[2] Baldwin, D. F.; Tate, D. E.; Park, C. B.; Cha, S. W.; Suh, N. P. Microcellular Plastics Processing Technology (2). *Seikei-Kakou* Vol.6, **1994**, pp. 245-256.
[3] Martini-Vvedensky, J. E.; Suh, N. P.; Waldman, F. A. Microcellular Closed Cell Foams and Their Method of manufacture. U.S. Patent #4,473,665
[4] Shimbo, M.; Baldwin, D. F.; Suh, N. P. Cell Size Effects on the Mechanical and Viscoelastic Behavior of Microcellular Plastics (in Japanese). *Seikei-Kakou* Vol.6, **1994**, pp. 863-868
[5] Collias, D. I., Baird, D. G. Does a Microcellular Structure Improve the Modulus of Toughness of a Polymer Matrix? *ANTEC* **1992**, 1532-1534
[6] Curtzen, P.J. *Gefahren und Auswege* **1989,** 25-48
[7] RITE, NEDO report on "Research on alternative CFCs and HCFCs" **1998**
[8] Arefmanesh, A.; Advani, S.G. Diffusion Induced Growth of a Gas Bubble in a Viscoelastic Fluid. *Rheological Acta* Vol.30, **1991**, pp. 274-283
[9] Goel, S. K.; Beckman, E. J. Nucleation and Growth in Microcellular materials: Supercritical CO_2 as Foaming Agent. *AIChE J.* Vol.41, **1995**, pp. 357
[10] Colton, J. S.; Suh, N. P. The Nucleation of Microcellular Thermoplastics Foam: process Model and Experimental Results. *ASME PED*, Vol.20, **1986**, pp. 261-276
[11] Colton, J. S.; Suh, N. P. The Nucleation of Microcellular Thermoplastic Foam with Additives: Part I: Theoretical Considerations. *Polym. Eng. Sci.* Vol.27, **1987**, pp. 485-492
[12] Colton, J. S.; Suh, N. P. The Nucleation of Microcellular Thermoplastic Foam with Additives: Part II: Experimental Results and Discussion. *Polym. Eng. Sci.* Vol.27, **1987**, pp. 493-499
[13] Colton, J. The Production of Microcellular Foams in Semi-Crystalline Thermoplastics. *ANTEC* **1988**, 719-722
[14] Kumar, V.; Suh, N. P. Production of Microcellular Plastic Parts. *ASME AMD* Vol.104, **1989**, pp. 321-339
[15] Kumar, V.; Weller, J.; Hoffer, H.-Y. Synthesis of Microcellular Polycarbonate: A Phenomenological of Bubble Nucleation and Growth. *ASME AMD* Vol.19, **1990**, pp. 197-212
[16] Kumar, V.; Vander Wel, M. M. Microcellular Polycarbonate: Part II: Characterization of Tensile Modulus. *ANTEC* **1991**, 1406-1410
[17] Kumar, V.; Weller, J. E.; Montecillo, R. J. *Vinyl Technol.* Vol.14, **1992**, pp. 191-197
[18] Satish, K. G.; Beckman, E.J. Nucleation and Growth in Microcellular Materials: Supercritical CO_2 as Foaming Agent. *AIChE J.* 1995, *41*, 357-367
[19] Satish, K. G.; Beckman, E.J. Generation of Microcellular Polymeric Foams Using Supercritical Carbon Dioxide. I: Effect of Pressure and Temperature on Nucleation. *Polym. Eng. Sci.* Vol.34, **1994**, pp. 1137-1147
[20] Utracki, L. A. National Research Council Canada, 1998
[21] Otake, K.; Sako, T.; Sugeta, T.; Yoda, S.; Takebayashi, Y.; Nakazawa, N.; Kamizawa, C. Proceedings of 5th Internat. Symp. on Supercrit. Fluids, Atlanta (USA), 2000
[22] Surat, A.; Nagamine, S.; Oshima, M.; Tanigaki, M. *Proceeding of the 32nd Autumn Meeting of the Society of Chemical Engineers, Japan*, **1999**, V303
[23] Ohyabu, H.; Otake, K.; Hayashi, H.; Inomata, H.; Taira, T. Proceeding of Polymer Processing Society 19th Annual meeting, Melbourne (Australia), 2003
[25] Ohoshima *et al.*, Proceeding of 38th annual meeting of Chemical Society of Japan, 2002
[24] Sato, Y.; Sorakubo, A.; Takishima, S.; Masuoka, H. Proceedings of 9th APCChE Congress and CHEMECA, New Zealand, 2002